Trans-Pacific transport of Saharan dust to western North America: A case study

Ian G. M^{c}Kendry
Atmospheric Science Program, Department of Geography, University of British Columbia, Vancouver, Canada

Kevin B. Strawbridge
Science and Technology Branch, Environment Canada, Centre for Atmospheric Research Experiments, Egbert, Ontario, Canada

Norman T. O'Neill
CARTEL, Department de Geomatique Appliquee, Université de Sherbrooke, Sherbrooke, Quebec, Canada

Anne Marie Macdonald
Science and Technology Branch, Environment Canada, Toronto, Ontario, Canada

Peter S.K. Liu
Science and Technology Branch, Environment Canada, Toronto, Ontario, Canada

W. Richard Leaitch
Science and Technology Branch, Environment Canada, Toronto, Ontario, Canada

Kurt G. Anlauf
Science and Technology Branch, Environment Canada, Toronto, Ontario, Canada

Lyatt Jaegle
Department of Atmospheric Sciences, University of Washington, Seattle, WA, USA

T. Duncan Fairlie
NASA Langley Research Center, Hampton, VA/ Dept. Earth and Planetary Sciences, Harvard University, Cambridge, MA, USA

Douglas L Westphal
Marine Meteorology Division, Naval Research Laboratory, Monterey, U.S.A.

INDEX TERMS: 0322 Atmospheric Composition and Structure: Constituent sources and sinks; 0368 Atmospheric Composition and Structure: Constituent Transport and chemistry; 3367 Meteorology and Atmospheric Dynamics: Theoretical modelling

KEYWORDS: Intercontinental Dust Transport, Saharan dust pathway, Tropospheric aerosol

Abstract

The first documented case of long range transport of Saharan dust over a pathway spanning Asia and the Pacific to Western North America is described. Crustal material generated by North African dust storms during the period 28 February – 3 March 2005 reached western Canada on 13-14 March 2005 and was observed by lidar and sunphotometer in the Vancouver region and by high altitude aerosol instrumentation at Whistler Peak. Global chemical models (GEOS-CHEM and NRL NAAPS) confirm the transport pathway and suggest source attribution was simplified in this case by the distinct, and somewhat unusual, lack of dust activity over Eurasia (Gobi and Takla Makan deserts) at this time. Over western North America, the dust layer, although subsiding close to the boundary layer, did not appear to contribute to boundary layer particulate matter concentrations. Furthermore, sunphotometer observations (and associated inversion products) suggest that the dust layer had only subtle optical impact (Aerosol Optical Thickness (τ_{a500}) and Angstrom exponent ($\alpha_{440\text{-}870}$) were 0.1 and 1.2 respectively) and was dominated by fine particulate matter (modes in aerodynamic diameter at 0.3 and 2.5 μm). High Altitude observations at Whistler BC, confirm the crustal origin of the layer (rich in Ca^{++} ions) and the bi-modal size distribution. Although a weak event compared to the Asian Trans-Pacific dust events of 1998 and 2001, this novel case highlights the possibility that Saharan sources may contribute episodically to the aerosol burden in western North America.

1. Introduction

Mobilisation and transport of mineral dust from the arid regions of the world is of considerable scientific importance due to the role airborne crustal material plays in the global radiation balance (and hence climate forcing), cloud processes, atmospheric chemistry, oceanic biogeochemical processes (e.g. dust is a major source of iron), as vectors for microbes and as a factor influencing local air quality in both "source" and "sink" regions (Prospero et al. 2002). In light of this, considerable effort, including observation, major field experiments and modelling, has been directed at the quantification of the sources and sinks of mineral dust as well as the major pathways by which dust is transported in the atmosphere (e.g. Ginoux et al. 2004).

Globally, the deserts of North Africa and Asia represent the major sources of mineral dust with North Africa (including the Sahara and Sahel) contributing about 1400 Tg/year (65% of the global emission) while the deserts of Asia (including the Gobi and Takla Makan deserts) contribute around 25% (Ginoux et al. 2004). From North Africa, mineral dust is transported principally along three pathways: (1) westward across the Atlantic to the Americas (2) northward across the Mediterranean to Europe and (3) eastward across the eastern Mediterranean to the Middle East and Asia. The latter trajectory, which is of particular relevance to this study, is most prevalent during spring (Middleton and Goudie, 2001). From Asia, the major transport pathway is eastward on the mid-latitude westerlies to the North Pacific (Prospero et al. 2002, Gong et al. 2003, Stohl et al. 2002, Holzer et al. 2003, 2005). The provenance of deposited dust demonstrates that the mid-latitude

westerlies episodically carry Asian dust as far afield as both the east and west coasts of North America (Husar et al., 2001, McKendry et al., 2001, Jaffe et al. 2003) and the European Alps (Grousset et al. 2003). Ice cores from Greenland suggest that this pathway has been active for a long period of time (Biscaye et al. 1997).

Modelling studies (Ginoux et al. 2004) indicate that North America is the only continent (Antarctica excluded) for which annual dust deposition exceeds emissions (by three fold). Hence long range transport from other continents is the dominant factor controlling the magnitude and interannual variability of dust loading. The primary pathway for intercontinental transport to North America is trans-Atlantic transport of North African dust, primarily to the eastern and south eastern USA, including the Caribbean (Chiapello et al. 2005). Recently Asia has been identified as a source affecting primarily the western USA (Husar et al. 2001, McKendry et al. 2001) and occasionally the entire continent (Jaffe et al. 2003; Thulasiraman et al. 2002).

In this study, we describe a previously undocumented pathway for long range transport of mineral dust to North America; eastward transport of North African dust across Eurasia and the North Pacific to western North America. In so doing we draw extensively upon available surface observations and remote sensing data (including lidar observations and sunphotometer data), as well as global meteorological and chemical models. Data from non-routine observations (AERONET site and High Altitude Chemistry site) permit examination of some physico-chemical characteristics of airborne dust at a considerable distance from source. This paper extends the study of Park et al. (2005) that attributes

lidar observed dust layers over Japan and China during the same time period (early March 2005) to dust storms in the Sahara region.

2. Methods

Examination of this case was prompted by West Coast North America arrival of a mid tropospheric mineral dust layer around 13 March 2005 as forecast by the NAAPS (Navy Aerosol Analysis and Prediction System) Global Aerosol Model (available at http://www.nrlmry.navy.mil/aerosol/) and observed by a continuous upward-pointing lidar at Vancouver, BC (lat 49°15'N, long 123°08'W) on 13-14 March 2005. As for the analysis of the 1998 Asian dust event (Husar et al. 2001), detailed examination of this case exploits a wide range of data products, including routine observations and models, many of which are available online.

The Environment Canada, Centre for Atmospheric Research Experiments (CARE) mobile lidar laboratory RASCAL (Rapid Acquisition SCanning Aerosol Lidar), was located at the University of British Columbia, Vancouver (Figure 1) in March 2005 in order to observe potential Asian dust transport events (see Strawbridge et. al. (2004) for a detailed description of RASCAL). For this application, RASCAL was operated in upward pointing mode (i.e. vertically sampling the atmosphere directly above the vehicle) rather than scanning mode. The vehicle has an electronic leveling system to provide a stable, level environment for lidar operation. The technique of lidar is essentially a time-of-flight experiment that provides high spatial and temporal resolution imagery of the atmosphere. The basic components of a scanning lidar system consist of a laser, beam

directing/collection optics and a telescope with a detection package to convert the signal for a data acquisition system that can process, display and save the data in real-time. A pulsed laser emits a burst of photons into the atmosphere. A detection system measures the amount of light scattered back from the particles in the atmosphere. The analog signal from the detector is digitized along a set range (typically 12 km) providing a resolution of 3m along the beam axis. The detector employed was a 35.6 cm Celestron Schmidt-Cassegrain telescope with an 8 mrad field-of-view that focused the captured light on a 3 mm RCA 30956E avalanche photodiode (APD). The APD was connected to a logarithmic amplifier made by Optech Inc. to increase the dynamic range. This is particularly important when operating the lidar where aerosol concentrations vary significantly within the scan range. The amplifier was calibrated prior to the experiment via a transfer function to convert the signal to a linear scale in addition to second order corrections provided by Optech Inc. The signal was then sent to a Gage 14-bit, PCI card where the information was digitized at 50 MHz (3m resolution along the beam axis). The laser was a Continuum Powerlite 8020 Nd:YAG with a measured output energy of 850mJ and 400mJ at 1064nm and 532nm respectively. The a-scope display and false-colour backscatter ratio plots are shown in real-time with the ability to zoom in and out during data collection.

The mineral dust simulation described here was conducted using the GEOS-CHEM chemical transport model (CTM) (Bey et al. 2001, Park et al., 2004). The model is driven by GEOS-4 assimilated meteorological fields provided by the NASA Global Modeling and Assimilation Office (GMAO) which include wind, temperature, pressure,

convective mass fluxes, precipitation fluxes, boundary layer height, and surface characteristics such as soil moisture, snow depth, and surface roughness. The meteorological fields used for the simulation have a horizontal resolution of 2.5^{o} by 2^{o} horizontal resolution, and 30 vertical levels extending from the surface to approximately 0.01 mb. Constituent advection is conducted in GEOS-CHEM using the flux-form semi-Lagrangian scheme of Lin and Rood (1996); sub-grid-scale convection is achieved using the scheme of Allen et al. (1996a,b).

The mineral dust module in GEOS-CHEM describes the mobilization (emission) of dust from the Earth's surface, large-scale transport by the wind, sub-grid-scale convective lofting, gravitational settling, and wet and dry deposition. For dust mobilization, GEOS-Chem uses the Dust Entrainment and Deposition (DEAD) scheme (Zender et al. (2003)). The mobilized mineral dust is distributed across four size bins for transport and deposition, with effective radii of 0.7, 1.4, 2.4 and 4.5 μm, following the approach of Ginoux et al. (2001). To compute optical properties, the smallest size bin is subdivided into four classes with effective radii of 0.15, 0.25, 0.4 and 0.8 mm. Dry deposition of dust is represented using a deposition velocity that accounts for gravitational settling (Seinfeld and Pandis, 1998) and turbulent dry transfer to the surface (Zhang et al., 2001). Wet deposition of mineral dust is represented using the parameterization for aerosol scavenging described by Liu et al. (2001), which includes scavenging in sub-grid-scale convective updrafts, and rainout and washout from large-scale precipitation and convective anvils. The coupled GEOS-CHEM ozone-aerosol model is run daily in near

real time, and results are available online: http://coco.atmos.washington.edu/cgi-bin/ion-p?page=geos_nrt.ion.

Independent corroboration of the GEOS-CHEM results is provided by the Navy Aerosol Analysis and Prediction System (NAAPS), the U.S. Navy's global operational aerosol, air quality and visibility forecast model that generates real-time forecasts of aerosol conditions worldwide (http://www.nrlmry.navy.mil/aerosol/). At 00Z and 12Z each day, NAAPS produces global dust, sulphate, and smoke forecasts on a 1 X 1 degree grid and 27 vertical levels out to six days using meteorological fields from the Navy Operational Global Atmospheric Prediction System (NOGAPS, the Navy's global weather model.) Both NOGAPS and NAAPS are run operationally at the Fleet Numerical Meteorology and Oceanography Center.

Back-trajectories from Vancouver were calculated using the HYSPLIT (HYbrid Single-Particle Lagrangian Integrated Trajectory) model (http://www.arl.noaa.gov/ready/hysplit4.html). The model is the newest version of a complete online system for computing simple air parcel trajectories to complex dispersion and deposition simulations for any location and date (depending on data availability) using a variety of standard data input products (e.g. the NCEP Reanalysis 1948-present). Further details and validation of the model can be found in Draxler and Hess (1998).

The AERONET (AErosol RObotic NETwork) program is an inclusive federation of ground-based remote sensing aerosol networks whose objectives include the

characterization of columnar aerosol optical properties as well as the validation aerosol optical parameters retrieved from the inversion of satellite radiances (http://aeronet.gsfc.nasa.gov/index.html). The network employs CIMEL sunphotometers / sky radiometers for the retrieval of information on aerosol optical properties. This type of information has been important in tracing the transport and characteristics of different types of aerosols and in particular has provided insight into the trans-Pacific transport of Asian dust. A CIMEL device on Saturna Island (Figure 1), a key site in a previous Asian dust study (Thulasiraman et al. 2001) was employed for similar purposes in this study. This site, a member of AEROCAN (the Canadian subnetwork of AERONET), is located approximately 50 km southwest of Vancouver. The CIMEL instruments acquire solar radiances which are transformed into cloud screened (level 1.5) Aerosol Optical Thickness (AOT) across seven spectral channels (340, 380, 440, 500, 670, 870, and 1020 nm) and, in a separate mode, almucanter sky radiances across four channels (440, 670, 870, and 1020 nm). The sky radiances, along with AOT estimates at the same four channels, are used to perform inversions for particle size distribution and refractive index (Dubovik et al., 2000). In this paper we examine (1) AOT at 500 nm (τ_{a500} or τ_a for simplicity): the fundamental aerosol parameter which acts to reduce the optical transmission in the direction of the sun and increases the brightness of the sky away from the sun (as τ_a increases the sky becomes hazier) (2) the partition of the AOT into its fine and coarse mode optical depths at 500 nm (τ_f and τ_c) and (3) particulate matter size distributions obtained from the Dubovik inversions. It should be borne in mind that the fine mode fraction (τ_f / τ_a) is proportional to the Angstrom exponent (O'Neill et al.,

2003); we simply choose to represent this key spectral parameter in terms of the more physically relevant fine and coarse mode contributions.

Measurements of particles and trace gases are made by Environment Canada at a high elevation site in Whistler, BC, approximately 100 km north of Vancouver (Figure 1). The site is located at the top of a ski hill, at Whistler peak, 2182 m (above sea level). There are no continuous combustion sources at the peak and influences from snowmobiles have been identified and removed from the data set. During the period of interest, particle size distributions were measured both with a TSI Scanning Mobility Particle Sizer (SMPS) Model 3934 and a Grimm optical particle counter (OPC) (Model 1.108). The SMPS was used to measure mobility diameter in the 0.01 μm to 0.4 μm size range while the OPC provided optical diameter from 0.3 μm to 20 μm. Particle chemistry is from bulk filter packs, collected every 48 hours and analyzed for inorganic ions by ion chromatography. All particle sampling takes place through a heated stainless steel manifold and filter packs are preceded by a cyclone operated at approximately a 2μm size cut. Particle sampling is suspended in the presence of fog to ensure no contamination of samples by cloud and that the sampling inlet remains dry and free of rime. Carbon monoxide is measured with a TECO 48C with zeros performed every two hours.

3. Results

3.1 Observed Dust Storms

During late February and early March 2005 significant dust storm activity was observed across the northern Sahara and in particular in the vicinity of Western Algeria (see http://www.nrlmry.navy.mil/aerosol/ for archived maps showing surface observations). This activity was visible in satellite imagery showing prominent veils of dust transported northeastward across Libya and Egypt into the eastern Mediterranean and beyond (Figure 2). These events were entirely consistent with the sources, trajectories and seasonality of North African dust events as described in great detail in Middleton and Goudie (2001). At other times of year, particularly summer, the subtropical easterly jet and easterly waves predominate over the region and tend to carry dust on a pathway extending westward across the Atlantic (Middleton and Goudie, 2001).

In contrast, during early March 2005, dust storm activity in the Asian Region was confined to slight to moderate activity in north western China over the period 6-10 March (see http://www.nrlmry.navy.mil/aerosol/ for archived maps showing surface observations). Generally by March, dust storm activity in Asia reaches a maximum as spring cyclonic storms from Siberia bring frontal activity and strong winds to the region (Prospero et al. 2002). However, early March 2005 was influenced by a well developed ridge of high pressure over central Asia and a pronounced absence of cyclonic activity (GEOS-CHEM simulations show transport over this ridge in the Asian region and absence of dust generated near the surface). It is this lack of activity over Asia which adds considerable weight to the view that dust arriving in North America on 13-14 March originated from Africa and was “uncontaminated” by Asian sources.

3.2 Transport: Meteorology

In this case, Saharan dust generation and eastward transport was associated with the passage of a relatively weak low pressure centre (~100hPa central pressure) eastward across North Africa accompanied by strong zonal mid- tropospheric westerlies (this transport can be seen in GEO-CHEM simulations shown in Figure 3 below). The short wave trough accompanying this system moved eastward across the eastern Mediterranean by 3 March 2005. Meteosat imagery (not shown here) shows no indication of frontal cloud associated with this system and consequently, it appears that the system did not exhibit a well-developed warm conveyer belt (WCB), the main mechanism by which pollutants are lofted to the mid-troposphere in mid-latitudes (Cooper et. al. 2004). Instead, it seems (based on comparison of GEOS-Chem simulations and weather maps) that lofting of dust to mid-troposheric levels occurred in the vicinity of the central core of the low pressure centre (and in advance of the developing shortwave trough) over Algeria and Libya as the system moved eastward on 28 February and 1 March 2005. In Figure 2 (top centre) dust is apparent above cloud confirming lofting of material into the mid-troposphere relatively near the source region.

Long-range transport of the Saharan dust is shown in Figure 3 (based on GEOS-CHEM simulations) with meteorological fields superimposed. The hemispheric long waves during the event showed a broadly three wave pattern with ridges over western North America, central Asia and the central Atlantic. This zonal pattern facilitated relatively rapid mid-tropospheric eastward transport, firstly over the central Asian ridge by 5 March, across the central Pacific by 9-11 March and finally across the western North American ridge during 12-14 March 2005. Over this trajectory, three cyclonic systems

affected transport: dust was first lofted in the low pressure centre over the Sahara, it then travelled around the southern portion of a mid-latitude cyclone in the eastern Pacific (7-9 March) and then around the south side of low pressure system in the eastern Pacific (11 March) before "pooling" north of Hawaii and then arching northward onto the north American continent. This pattern is consistent with research by Cooper et al. (2004) and Holzer et al. (2004) that suggests that several baroclinic systems need to "cooperate" in order to generate trans-Pacific transport events.

During the long hemispheric trajectory described herein, significant precipitation and cloud was associated with only the eastern and western Pacific mid-latitude cyclones with no significant precipitation associated with the Asian leg of the pathway. Comparison of the left and right panels in Figure 3 suggests that during transport across the Pacific, the core of the dust layer avoided regions of precipitation (and therefore significant wet deposition) associated with low pressure centers in the northern Pacific.

3.3 Transport: GEOS-CHEM Simulations of Dust Optical Depths

Dust optical depths (computed at 400nm) in Figure 3 show both surface sources and dust storm activity as well as mid-tropospheric transport. Throughout the period, significant surface dust mobilisation events were limited to 28 February – 7 March 2005 over North Africa with little or no activity of Asia. The most intense activity is evident over Western Algeria on 28 February and is consistent with satellite imagery (Figure 2) and surface reports over the region.

By 3 March, north-eastward transport of North African dust is evident over the Middle East. This pathway follows the middle latitude westerlies across the ridge over central Asia and dips southward across East Asia and Japan into the Pacific by 7 March.

Confirmation of the transport of mid tropospheric dust layers across China and Japan 7-9 March 2005 is provided by lidars in the region. Park et al. (2005) attribute these layers to North African dust storms (26 Feb – 2 March 2005) on the basis of results from five regional and global aerosol models. In their study, global models reproduced the dust layer qualitatively, but the regional model did not. Consequently, it was concluded that the source of the dust layers was located outside the regional model domain that included the Taklimakan and Gobi Deserts. As with the GEOS-CHEM model described herein, the global models (including NRL NAAPS) showed the plumes originating from the Sahara Desert, with models showing no major dust emission in the Taklimakan and Gobi Deserts during the period.

Across the Pacific, the GEOS-CHEM simulation shows strongly zonal flow until the dust reaches a point northward of Hawaii around 9 March, at which time it arches northward over the strong ridge along the west of the Pacific coast of North America. The leading edge of the Saharan dust reaches Vancouver on 13 March and represents a total transport duration of ~14 days. Latitudinal cross-sections (not shown here) along the transport pathway indicate that transport was mid-tropospheric for the entire event and suggests that on arrival in the Vancouver region on 13 March the centre of the dust layer was at ~5-6km altitude. Over Japan and China simulated heights of the dust layer are consistent with lidar observed layers described by Park et al. (2005).

3.4 Observations over western North America

Continuous upward pointing lidar imagery from Vancouver, British Columbia on 13 March 2005 shows a layer of enhanced backscatter at approximately 5km AGL in the morning (marked A in Figure 4a) that is entirely consistent with the GEOS-CHEM simulations. This aerosol layer progressively lowered throughout the remainder of 13 March and by early morning on 14 March it was located just above the planetary boundary layer at ~2km AGL, where it persisted for the remainder of the day. During 14 March the lidar imagery shows little evidence of down-mixing (or fumigation) of this layer. This is confirmed by surface monitoring in the vicinity of Vancouver showing little evidence of crustal material within the boundary layer over the period 12-14 March. At Vancouver International Airport mean concentrations for PM_{10} and $PM_{2.5}$ were 18 and 7 μgm^{-3} respectively. This represents "clean air" in the Vancouver context and compares to values which were approximately five times greater during the 1998 Asian dust event (McKendry et al. 2001; McKendry, 2000). Peak values were evident overnight and corresponded to peaks in CO. This suggests an anthropogenic local source for fine particles in the boundary layer over this period. Weather conditions on 13 March were mainly clear with temperatures reaching 14^{o}C at Vancouver International Airport. On 14 March temperatures reached 13^{o}C with altocumulus cloud present until early afternoon. This cloud is apparent in the lidar imagery (label B in Figure 4). The corresponding NAAPS forecast aerosol extinction for Saturna Island over the same period is shown in

Figure 4b (time and height scales are matched to allow direct comparison). The model forecast shows remarkable agreement with the observations, capturing not only the height and arrival time of the dust layer, but also the significant subsidence that occurred over the night of 13/14 March 2005.

Hysplit back trajectories (Figure 5) for multiple elevations suggest that the air mass passing over Vancouver during this episode had followed an arching northerly trajectory over the well developed ridge of high pressure aligned westward of the West Coast. This is consistent with the trajectories shown in the GEOS-CHEM simulations above (Figure 3). Interestingly, the trajectory starting at 1km (in red) can be traced back to the mid troposphere (~5km), the height at which dust was predicted to traverse the Pacific by the GEOS-CHEM and NAAPS models. This is consistent with the notion that strong subsidence on the eastern limb of the upper level ridge was likely responsible for the lowering of the elevated layer apparent in the lidar imagery.

The Saturna Island sunphotometer data appears to confirm the presence of enhanced aerosol over the region on 13-14 March 2005, however the optical effects of the mineral dust were subtle compared to the spectacular Asian Dust Episodes of April 1998 (Husar et al. 2001) and mid-April 2001 (Jaffe et. al. 2003; Thulasiraman et al. 2001). Figure 6a shows the variation of total AOD and predicted (NAAPS) dust AOD for AEROCAN/AERONET data acquired on Saturna Island (500 nm wavelength). Although the correlation between the model and data is not strong its interpretation as being indicative of the dust event is convincing given (for example) the sudden increase to

smoothly varying measured optical depth on March 13, low values of τ_f / τ_a (or equivalently, high values of τ_c / τ_a where one assumes that dust events always have a strong coarse mode component) and circumstantial evidence such as the correspondence with lidar and microphysical data. Figure 6b shows the estimated values of τ_f and τ_c extracted from the spectral form of the total AOD. These curves enable one to better understand those variations in the measured optical depths which tend to lessen the correlation with the modelled dust optical depth. The blue vertical lines indicate probable thin-cloud events or thin cloud events combined with dust intrusions where the cloud component likely escaped the AERONET cloud screening algorithm (Smirnov et al., 2000). If one roughly defines a high frequency minimum for cloud optical depth variation as the maximum dust rate derived from the NAAPS data of Figure 6a then a threshold temporal rate for thin cloud would be $d\tau_c / dt >\sim 0.02$ / hour. While this frequency argument will have some sensitivity to the nominal sampling frequencies of the model, there are clearly fundamental differences between the temporal behavior of local (low altitude) cloud and well travelled dust. As opposed to the more obvious dust signal on Mar. 13, the variations of τ_c on 9 March and 14 March suggest a mixture of cloud and dust influences (38% of all the point pairs on 9 March and 28% of all the point pairs of 14 March respectively would be classified as cloud according to the temporal derivative criterion given above). The last pair of (red) vertical lines on Mar. 24 and 25 show a fine mode optical depth variation which is likely a local pollution event (c.f. the Whistler analysis below).

The size distribution derived by inversion for the 12-14 March 2005 period (whose daily average is shown in Figure 7) suggests that arrival of dust on 13 March was associated with a significant increase in particle volume (and likely mass) at a mode of 0.3 μm aerodynamic diameter and a lesser increase in the coarse mode at around 2.5 μm. It will be seen in the analysis of the Whistler data below that the relative importance of the fine and coarse mode peaks is somewhat at odds with the sampled particle size distributions (where the coarse mode volume size distribution is significantly more important in the 13/14 March data of Figure 9 versus the 13/14 March data of Figure 7). Aside from the obvious sources of potential disparities (column integration versus local volumetric sampling and the distance between the Vancouver area sites and Saturna Island) one can easily demonstrate a significant variability of the fine mode volume size distribution as a function of the retrieved value of refractive index as well as the assumption of non-sphericity versus sphericity of the dust particles (the fine mode particle volume being significantly less, for example, in the case of a retrieval based on the assumption of non-spherical particles; see Dubovik et al. 2002b). In contrast, the coarse mode volume distribution is considerably less sensitive to these retrieval parameters. The refractive index is not, as a matter of fact, even returned by the AERONET inversion because the authors of the algorithm do not recommend its use below $\tau_a(440\ nm) < 0.5$ for dust particles (the refractive index remark above is based on our own Mie computations applied to the Mar. 2005 dust data).

The implied correlation between fine and coarse mode dust content seen in Figure 7 is coherent with the moderate correlation which can be seen between the τ_f and τ_c curves of

Fig. 6b on Aug. 13 when the influence of the dust intrusion was most evident. That this correlation is actually due to a dominance of dust in the fine mode as opposed to a dominance of anthropogenic local sources is not clear (see the Vancouver airport and Whistler analyses below). Nonetheless, the existence of both fine and coarse dust modes is similar to previous sunphotometry-derived results for Asian Dust over Alaska, British Columbia and coastal California (Stone et al.(2005); Table 3 of Thulasiraman et al. (2001); Tratt et al. (2000) respectively) as well as Saharan dust transported westward to Cape Verde (Dubovik et al. (2002a); Tanré et al. (2001)) and was observed by McKendry et al. (2001) using volumetric sampling techniques in the Vancouver area during the strong 1998 dust event. It is noted that the correlation between dust volume concentrations of the fine and coarse mode (i.e. C_{vf} and C_{vc} retrieved from integrations of the Dubovik particle size distributions) with τ_a(1020 nm) as presented in Table 1 of Dubovik et al. (2002a) and Table 3 of Thulasiraman et al. (2001) depends on there being significant variations in dust abundance during a given event; a lack of strong variation (as in the present case study) as well as ambiguity as to the nature of the fine mode variation (dust versus local anthropogenic) becomes problematic in the case of C_{vf} which is much more sensitive, as indicated above, to the retrieval conditions.

The position of the smaller coarse mode peak in Fig. 7 has been observed for Asian dust results over Hawaii and North America (Shaw, 1980; Stone et al., 2005; Thulasiraman et al., 2001; Tratt et al., 2000) as well as for Saharan dust over Cape Verde (Dubovik et al. (2002a); Tanré et al. (2001)). Shaw argued, as have subsequent authors (see Tratt et al., 2000 for example), that large ($r > 5$ μm) dust particles were depleted by the depositional

effects of long range transport. The average geometric volume mean radius (r_{vc}) for the 13 March measurements is a little larger than reported values (~ 1 - 2 μm radius) because it includes the second, larger-diameter coarse mode peak seen in Fig. 8. While it is unlikely that this second peak is of dust origin, the marginal optical signals in the present analysis preclude any definitive conclusion (the two course-mode volume concentrations are in fact correlated on Mar. 13 but an inversion artifact cannot be excluded).

At the Whistler high altitude station, particle measurements (Figure 8a-c) for the period show a major peak 13-15 March, a slightly lesser peak 9-10 March and a third peak 23-25 March 2005. The different characteristics of these events are evident from the time series of particle volume distributions (Fig 8a), which show significant coarse mode aerosol throughout the 9-10 March and 13-15 March events, yet not during 23-25 March. Also, while little particle volume is found in the accumulation mode 9-10 March, the 13-15 March and the 23-25 March events are completely dominated by accumulation mode aerosol (an observation consistent with the τ_f time series in Fig 6b). The time series of total particle volume above and below 1 μm geometric diameter (Fig 8b) suggests that the major peak 13 – 15 March reached a maximum around 1-2am LST on 14 March. This is consistent with the layer subsidence shown in the lidar imagery (i.e. the layer would have reached Whistler elevation at approx. this time). Average volume distributions over the peak period (13 March 2200 to 14 March 0600 LST) (Fig 8a and 9) are bimodal with the smaller mode at 0.3 μm and a larger mode at 2.5 μm diameter. This bimodal aspect of the distribution is in agreement with the sunphotometer data described above.

However, the SMPS/OPC measurements show the larger increase in volume occurs in the coarse mode rather than the accumulation mode. The volume distribution for 10 March (0000 – 0900 LST) is very similar to the 13-15 March period throughout the coarse mode, however there is no significant particle number or volume found in the accumulation mode. This is further illustrated by the particle sulphate ($SO_4^{=}$) and calcium (Ca^{++}) ions analyzed from the filter packs (Fig 8c). The particle chemical composition provides an important indication of the origin of particulate matter contributing to the particle events occurring at the high altitude station during March. Most notably, the increase in calcium during 9-10 March and 13-15 March is a strong indication of a crustal source. Low sulphate is observed during 9-10 March with an increase in particle sulphate during 13-15 March indicating some mixing of anthropogenic sources with the dust event. Carbon monoxide (Fig 8b) also increases by approximately 30 ppbv from the 9-10 March period to the 13-14 March period. The increase in this long-lived pollution tracer corresponds well with the increase in accumulation mode aerosol throughout these two periods. The two earlier periods are in contrast with 23-25 March which is characterized by low calcium and higher sulphate. This composition suggests a non-crustal source and results from local or regional pollution. It is important to note that because the filter packs were operated with a cut size of approximately 2 μm, they collected only a fraction of the coarse mode aerosol as estimated from Fig 9. Based on the GEOS CHEM simulations it is likely that the dust evident on 9-10 March was the forerunner of the event apparent on 13-15 March.

4. Discussion and Conclusions

A combination of global aerosol modelling output, as well as lidar, sunphotometer and high altitude surface monitoring observations confirm the presence of a dust layer over western North America on 13-14 March 2005. GEOS-CHEM and NAAPS simulations, together with an analysis of surface and satellite observations of dust storm activity in North Africa and Eurasia strongly suggest that this layer originated from significant dust storm activity in northwestern Algeria approximately 14 days earlier. The mineral dust followed a mid tropospheric pathway that crossed Asia and the Pacific and then gradually subsided in a ridge along the west coast of North America. This result is consistent with lidar observations and modelling studies for the same event as observed over Japan and China (Park et al. 2005). On the basis of sunphotometer data and surface observations in British Columbia it appears that this event had a weak but detectable impact on near surface PM concentrations and aerosol optical depths. However, the significance of the observations reported here rests on the fact that we have succeeded in identifying a case of very long range transport of dust (~19,000km) over an intercontinental pathway not previously documented. As such, this transport is of a similar importance to the documented cases of very long range transport of Asian dust to Greenland and the European Alps (Grousset et al. 2003; Biscaye et al. 1997) and ~17 day hemispheric transport of southeast Russian forest fire plumes (Damoah et al. 2004).

Further research is required to establish the frequency and magnitude of long range dust transport associated with this pathway. However, in this case, the occurrence and identification of the event arose due to a seemingly favourable combination of factors

that included (a) significant dust storms in Africa, (b) favourable mid-tropospheric meteorological conditions (rapid and direct transport in the mid – troposphere with little impact of precipitation) and (c) the somewhat unusual lack of significant dust activity in Eurasia to confound interpretation of sources. On this basis, it seems likely that such episodes are relatively rare, and when they do occur, have little impact on the aerosol burden in North America.

Finally, identification of this event would not have been possible without ready access to multiple data sources (model output, satellite imagery, surface monitoring observations and sunphotometer data) and the cooperation of scientists in several institutions. Consequently, this study again demonstrates that "*ad-hoc* collaboration of scientists is a practical way to share observations and to collectively generate the explanatory knowledge about such unpredictable events" (Husar et al. 2001).

Acknowledgements

We are grateful to Seane Trehearne (Totem Field Station) and Jan Patocka (Land and Building Services) of the University of British Columbia for lidar site access and preparation, and Michael Travis for lidar operations. The authors also acknowledge the commitment and valuable contributions of Gerri Crooks (Saturna Island site operator) and Jim Freemantle (AEROCAN coordinator). Research was support by grants from the Natural Sciences and Engineering Research Council of Canada. Thanks to Paul Jance for Figure 1, and two anonymous reviewers for constructive comments.

References

Allen, R.B. Rood, A. M. Thompson, and R. D. Hudson, Three-Dimensional Rn-222 Calculations Using Meteorological Data and a Convective Mixing Algorithm, *J. Geophys. Res.*, 101, 6871-6881, 1996.

Allen, D.J., P. Kasibhatla, A. M. Thompson, R. B. Rood, B. G. Doddridge, K. E. Pickering, R. D. Hudson, and S.-J. Lin, Transport-induced Interannual Variability of Carbon Monoxide Determined Using a Chemistry and Transport Model, *J. Geophys. Res.*, 101, 28655-28669, 1996.

Bey I., D. J. Jacob, R. M. Yantosca, J. A. Logan, B. Field, A. M. Fiore, Q. Li, H. Liu, L. J. Mickley, and M. Schultz, *Global modeling of tropospheric chemistry with assimilated meteorology: Model description and evaluation*, J. Geophys. Res., **106**, 23,073-23,096, 2001.

Biscaye, P.E., F.E. Grousset, M. Revel, S. Van der Gaast, G.A. Zielinsky, A. Vars and G. Kukla, Asian provenance of Last Glacial Maximum dust in the GISP-2 Ice core, Summit Greenland, *J. Geophys Res. 102*, 26, 765-781, 1997.

Chiapello, I., C. Moulin, and J.M. Prospero, Understanding the long-term variability of African dust transport across the Atlantic as recorded in both Barbados surface concentrations and large-scale Total Ozone Mapping Spectrometer (TOMS) optical thickness, *J. Geophys. Res.*, 110, D18S10, doi:10.1029/2004JD005132, 2005.

Cooper, O.R., C. Forster, D. Parrish, M. Trainer, E. Dunlea, T. Ryerson, G. Hübler, F. Fehsenfeld, D. Nicks, J. Holloway, J. de Gouw, C. Warneke, J. M. Roberts, F. Flocke, and J. Moody, A case study of trans-Pacific warm conveyor belt transport: The influence

of merging airstreams on trace gas import to North America, *J. Geophys. Res.* 109, D23S08, doi:10.1029/2003JD003624, 2004

Damoah, R., N. Spichtinger, C. Forster, P. James, I. Mattis, U. Wandinger, S. Beirle, and A. Stohl, Around the world in 17 days - hemispheric-scale transport of forest fire smoke from Russia in May 2003. *Atmos. Chem. Phys*. 4, 1311-1321, 2004.

Draxler, R.R. and G.D. Hess, An Overview of the HYSPLIT_4 Modelling System for Trajectories, Dispersion, and Deposition, *Australian Met. Mag.* 47, 295-308, 1998.

Dubovik, O., B. N. Holben, T. F. Eck, A. Smirnov, T. Lapyonok, A.Sinyuk, A.Vermeulen, D. Tanre , P.Goloub and I. Slutsker, Retrieval of Optical Properties of Desert Dust Aerosol from AERONET Observations, 2nd Workshop on Mineral Dust, Paris, France, September 10-12, 2003.

Dubovik, O., B.N.Holben, T.F.Eck, A.Smirnov, Y.J.Kaufman, M.D.King, D.Tanre, and I.Slutsker, Variability of absorption and optical properties of key aerosol types observed in worldwide locations, *J.Atm.Sci.,* **59**, 590-608, 2002a.

Dubovik, O., B.N.Holben,T. Lapyonok, A.Sinyuk, M. I. Mishchenko, P. Yang, and I.Slutsker, Non-spherical aerosol retrieval method employing light scattering by spheriods,*Geophys. Res. Lett.,* **29**, 54-1 - 54-4, 2002b.

Dubovik, O. and M. D. King, A flexible inversion algorithm for retrieval of aerosol optical properties from Sun and sky radiance measurements," *J. Geophys. Res.*, **105**, 20 673-20 696, 2000.

Ginoux, P., M. Chin, I. Tegen, J.M. Prospero, B. Holben, O. Dubovik, and S-J. Lin, Sources and distributions of dust aerosols simulations with the GOCART model, J. Geophys. Res., 106, D17, 20,255-20,273, 2001.

Ginoux, P., J.M. Prospero, O. Torres, and M. Chin, Longterm simulation of dust distribution with the GOCART model: Correlation with the North Atlantic Oscillation, *Environmental Modeling and Software, 19*, 113-128, 2004.

Gong, S.L., X. Y. Zhang, T. L. Zhao, I. G. McKendry and D. Jaffe, Characterization of soil dust aerosol in China and its transport/distribution during 2001 Ace-Asia period: Model simulation and validation," *J. Geophys. Res.* 108 4262,doi:10.1029/2002JD002633, 2003.

Grousset, F.E., P. Giroux, A. Bory, P.E. Biscaye, Case study of a Chinese dust plume reaching the French Alps, *Geophys. Res. Letts*, 30(6), 1277, 2003.

Hacker, J. P., I. G. McKendry and R. B. Stull, Modeled downward transport of Asian dust over Western North America during April 1998, *J. Appl. Met.*, 40, 1617-1628, 2001.

Holzer M., I.G. McKendry and D.A. Jaffe, Springtime Trans-Pacific atmospheric transport from East Asia: A transit-time-PDF approach. *J. Geophys. Res.*, 108, D22, 4708, 10.1029/2003JD003558, 2003.

Holzer, M. T.M. Hall and R.B. Stull, Seasonality and weather-driven variability of trans - Pacific transport, *J. Geophys. Res.,* 110, D23103, doi:10.1029/2005JD006261, 2005

Husar R.B., et al., The Asian Dust Events of April 1998. *J.Geophys. Res.* 106, 18,317-18,33, 2001.

Jaffe D., J. Snow , and O. Cooper, The April 2001 Asian dust events: Transport and substantial impact on surface particulate matter concentrations across the United States. *EOS transactions*. 84 (46), 501-507, 2003

Liang, Q., L. Jaeglé , and J. M. Wallace, Meteorological indices for Asian outflow and transpacific transport on daily to interannual timescales, *J.Geophys. Res.*, 110, D18308, doi:10.1029/2005JD005788, 2005.

Lin, S-J. and R. Rood, Multidimensional Flux-Form Semi-Lagrangian Transport Schemes *Mon. Wea. Rev.,* 124, 2046-2070, 1996.

Liu, H., .D.J. Jacob, I. Bey, and R.M. Yantosca, Constraints from ^{210}Pb and ^{7}Be on wet deposition and transport in a global three-dimensional chemical tracer model driven by assimilated meteorological fields, *J. Geophys. Res.,* 106 , 12,109-12,128, 2001

Middleton, N.J. and A.S. Goudie, Saharan Dust: Sources and Trajectories. *Transactions of the Institute of British Geographers*, 26, 165-181, 2001

McKendry, I.G., J. P. Hacker, R. Stull, S. Sakiyama, D. Mignacca and K. Reid, Long range transport of Asian dust to the Lower Fraser Valley, British Columbia, Canada, *J. Geophys. Res.*, 106(D16), p. 18361-18370, 2001.

McKendry, I. G., PM_{10} levels in the Lower Fraser Valley, BC, Canada: an overview of spatio -temporal variations and meteorological controls, *J. Air and Waste Manag. Ass.*, 50, p. 174-185, 2000

Park C.B., N. Sugimoto, I. Matsui, A. Shmizu, B. Tatarov, A. Kamei, C H Lee, I. Uno, T. Takemura, and D. L. Westphal, Long-Range Transport of Saharan Dust to East Asia Observed with Lidars, Scientific Online Letters on the Atmosphere (SOLA - http://www.jstage.jst.go.jp/browse/sola/1/0/_contents) 1, 121-124, 2005

O'Neill, N. T.,T. F., Eck, A. Smirnov, B. N.Holben, S. Thulasiraman, Spectral discrimination of coarse and fine mode optical depth, Vol.. 108, *J. Geophys. Res.,* No. D17, 4559-4573, 10.1029/2002JD002975, 2003.

Park, R. J., D. J. Jacob, B. D. Field, R. M. Yantosca, and M. Chin, *Natural and transboundary pollution influences on sulfate-nitrate-ammonium aerosols in the United States: implications for policy*, J. Geophys. Res., **109**, D15204, 10.1029/2003JD004473, 2004.

Prospero, J.M., P. Ginoux, O. Torres, S. Nicholson, and T. Gill, Environmental Characterization of Global Sources of Atmospheric Soil Dust Identified with the NIMBUS7 Total Ozone Mapping Spectrometer (TOMS) Absorbing Aerosol Product, *Rev. Geophys*., *40*, 1, 1002, doi:10.1029/2000RG000095, 2002.

Seinfeld and Pandis, 1998, Atmospheric chemistry and physics, John Wiley and Sons, Inc., New York

Shaw, G. E., Transport of Asian Desert Aerosol to the Hawaiian Islands, *Jour. App. Met*., Vol. 19, 1254-1259, 1980.

Smirnov A., B.N.Holben, T.F.Eck, O.Dubovik, and I.Slutsker, Cloud screening and quality control algorithms for the AERONET data base, *Rem. Sens. Environ*., 2000.

Stohl, A., S. Eckhardt, C. Forster, P. James and N. Spichtinger, On the pathways and timescales of intercontinental air pollution transport, *J. Geophys. Res.* 107 (d23), 4684, doi:10.1029/2001JD001396, 2002.

Stone, R. , G. Anderson, E. Andrews, E. Dutton, J. Harris, E. Shettle, A. Berk, Asian Dust Signatures at Barrow: Observed and Simulated incursions and impact of Asian Dust over Northern Alaska, IEEE extended abstract in the April 2005 special workshop Proceedings in honor of John Reagan, U. Ariz., 2005.

Strawbridge, K.B. and Snyder, B.J. Planetary boundary layer height determination during Pacific 2001 using the advantage of a scanning lidar instrument. *Atmos Environ*. 38 (34): 5861-5871, 2004.

Tanré, D., Y. J. Kaufman, B. N. Holben, B. Chatenet, A. Karnieli, F. Lavenu, L. Blarel, O. Dubovik, L. A. Remer and A. Smirnov, 2001: Climatology of dust aerosol size distribution and optical properties derived from remotely sensed data in the solar spectrum. *J. Geophys. Res*., Vol. 106, No. D16, 18,205–18,217, 2001.

Thulasiraman, S., N. T. O'Neill, A. Royer, B. N. Holben, D. L. Westphal, and L. J. B. McArthur, Sunphotometric observations of the 2001 Asian dust storm over Canada and the U.S. *Geophys. Res. Lets*. 29(8), 10.1029/2001GL014188, 2002

Tratt, D. M., Frouin, R. J. ; Westphal, D. L. 2001 April 1998 Asian dust event: A southern California perspective, *J. Geophys. Res.*, Vol. 106 , No. D16 , p. 18,371 (2000JD900758), 2000.

Zender, C.S., H. Bian, and D. Newman, The mineral dust entrainment and deposition (DEAD) model: description and 1990's dust climatology, *J. Geophys. Res*., 108, 2003

Zhang, L., S. Gong, J. Padro, L. Barrie, A size-segregated particle dry deposition scheme for an atmospheric aerosol module, *Atmos. Environ*, 35, 549-560, 2001

Zhao, T.L., S.L. Gong, X.Y. Zhang, I.G. McKendry, Modelled size-segregated budgets of soil dust aerosol during ACE-Asia, 2001: Implications for Trans-Pacific transport, *J. Geophy. Res.* 108**,** 8665,doi:10.1029/2002JD003363, 2003

Figure Captions

Figure 1: Western Canada showing observation sites mentioned in text

Figure 2: Dust Veils streaming off North Africa 1 March 2005 (this image from the Moderate Resolution Imaging Spectroradiometer (MODIS) on NASA's Terra satellite). Available online at the NASA Earth Observatory: http://earthobservatory.nasa.gov/NaturalHazards/

Figure 3: Figure 3: Paired GEOS-CHEM output panels showing (a) left hand side, Dust Optical Depth with 500hPa geopotential heights and (b) right, surface pressure with modelled precipitation per day for the period 28 February – 13 March 2005.

Figure 4: Time-height cross-sections of (a) aerosol backscatter from lidar at Vancouver 13-14 March (times in GMT) and (b) NAAPS forecast aerosol extinction for Saturna Island for the same period (times in GMT). NB Both panels are aligned to be time and height consistent.

Figure 5: Hysplit 72 hour backward trajectories ending at Vancouver 14 March 2005 for three levels 1000, 2000 and 5000 m AGL.

Figure 6: AOD at Saturna Island (a) variation of total AOD and predicted (NAAPS) dust AOD for AEROCAN/AERONET data (b) estimated fine and coarse mode optical depths extracted from the spectral form of the total AOD

Figure 7: Aerosol size distributions derived by Saturna Sunphotometer inversion methods (daily averages) before (12 March) and during dust event.

Figure 8 (a) Time series of particle volume distributions (0.01 to 20 μm diameter) at the Whistler high elevation site. Plot shows dV/dlogD as a composite from the SMPS and OPC. White areas indicate missing data.
(b) Time series of sub-micron and super micron total particle volume as determined from the SMPS and OPC.
(c) Sulphate and calcium concentrations from filter packs for particles less than 2 μm diameter.

Figure 9: Number and volume distributions from the SMPS and OPC composites of Figure 8a averaged over selected periods (i) March 10 00:00 to 09:00, (ii) Mar13 22:00 to March 14 06:00, and (iii) Mar 24 08:00 to 20:00 LST.

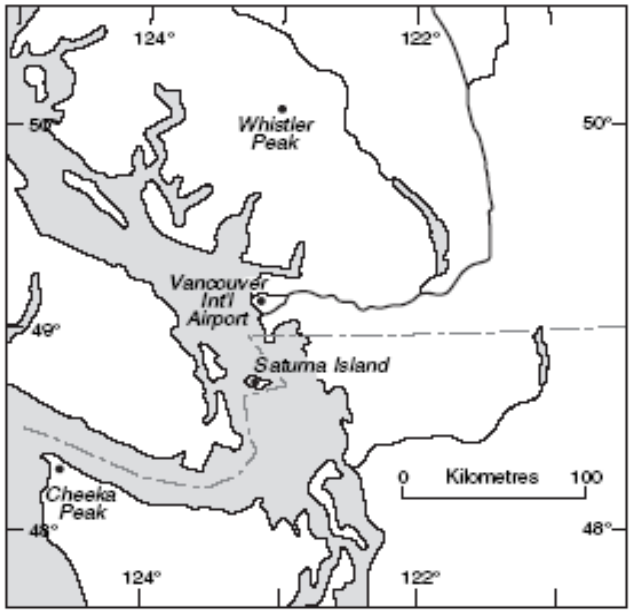

Figure 1: Western Canada showing observation sites mentioned in text

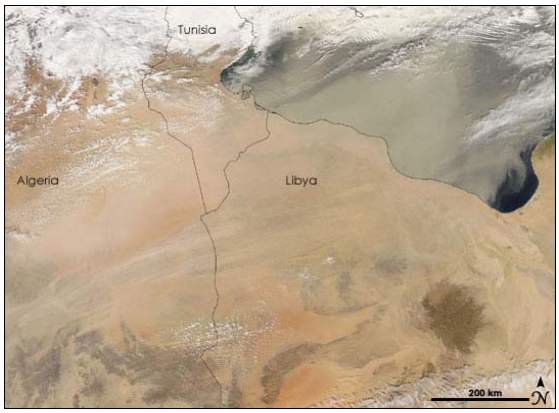

Figure 2: Dust Veils streaming off North Africa 1 March 2005 (this image from the Moderate Resolution Imaging Spectroradiometer (MODIS) on NASA's Terra satellite). Available online at the NASA Earth Observatory: http://earthobservatory.nasa.gov/NaturalHazards/

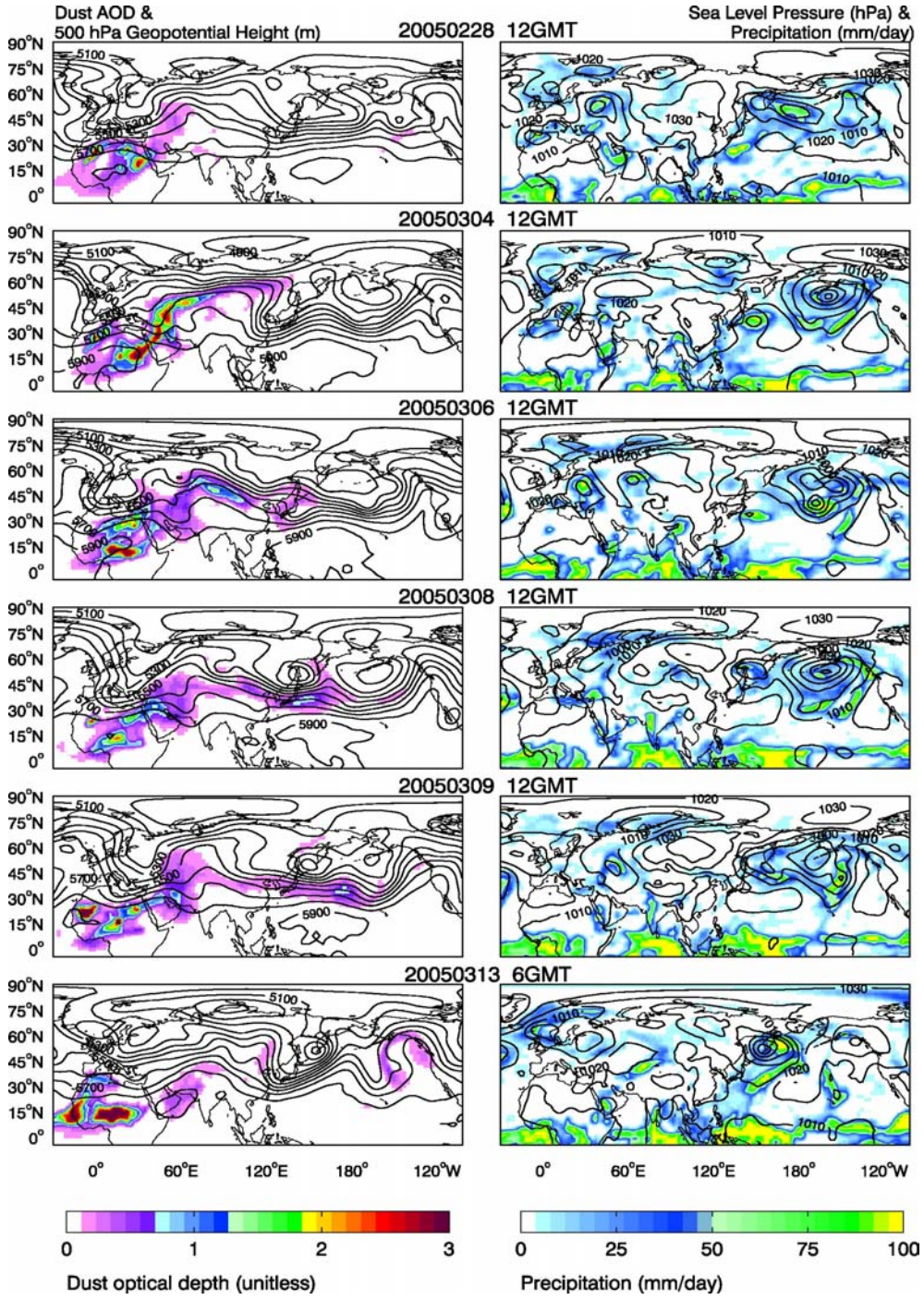

Figure 3: Paired GEOS-CHEM output panels showing (a) left hand side, Dust Optical Depth with 500hPa geopotential heights and (b) right, surface pressure with modelled precipitation per day for the period 28 February – 13 March 2005.

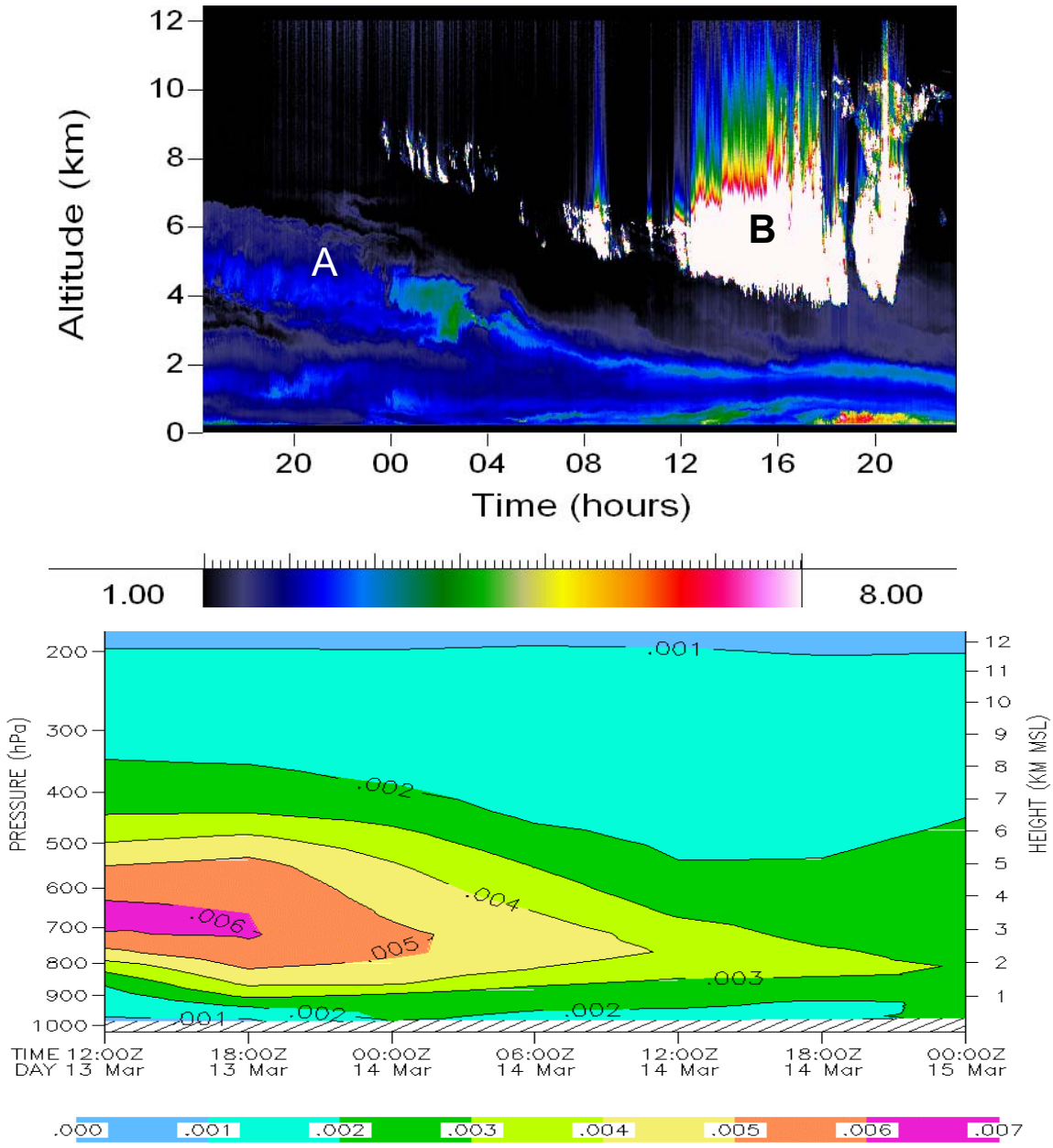

Figure 4: Time-height cross-sections of (a) aerosol backscatter from lidar at Vancouver 13-14 March (times in GMT) and (b) NAAPS forecast aerosol extinction for Saturna Island for the same period (times in GMT). NB Both panels are aligned to be time and height consistent.

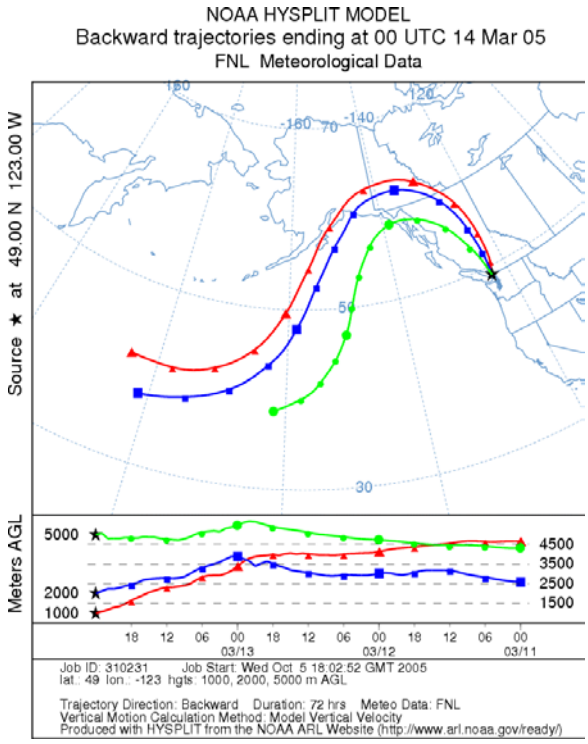

Figure 5: Hysplit 72 hour backward trajectories ending at Vancouver 14 March 2005 for three levels 1000, 2000 and 5000 m AGL.

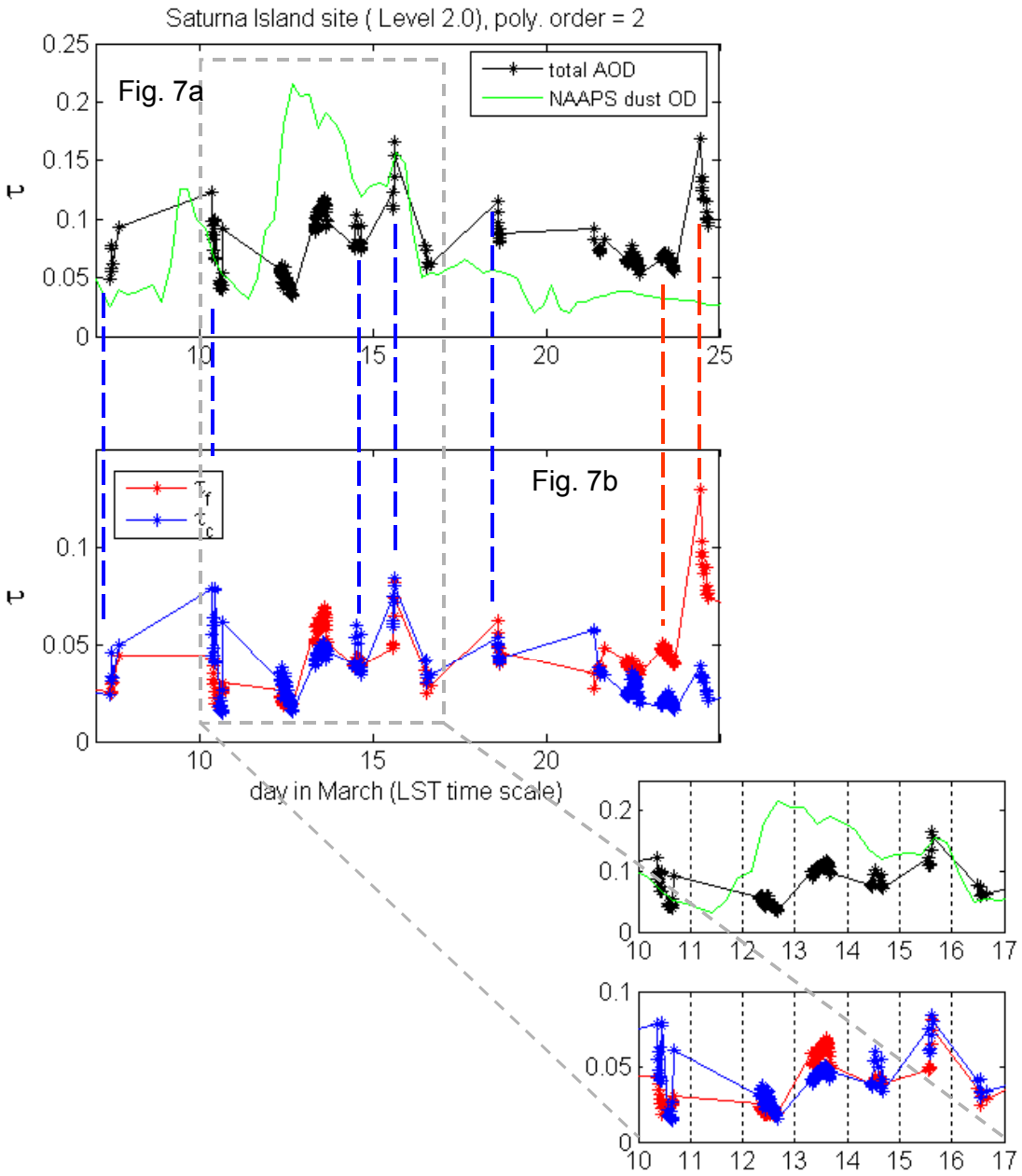

Figure 6: AOD at Saturna Island (a) variation of total AOD at 500 nm and predicted (NAAPS) dust optical depth for AEROCAN/AERONET data (b) estimated fine and coarse mode optical depths extracted from the spectral form of the total AOD

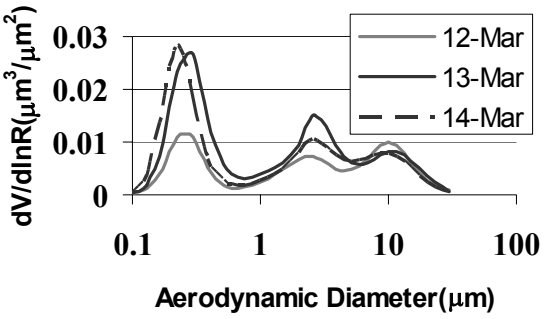

Figure 7: Aerosol size distributions (daily averages) derived by Saturna Sunphotometer inversion methods before (12 March) and during dust event.

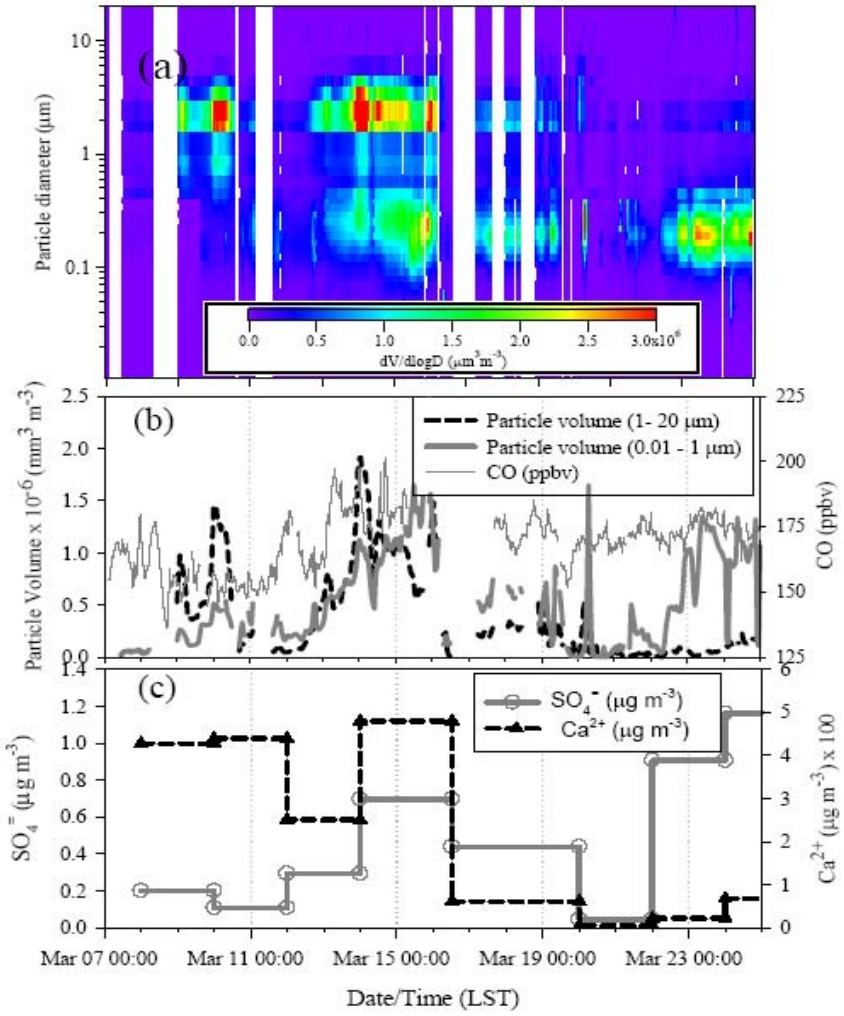

Figure 8: (a) Time series of particle volume distributions (0.01 to 20 µm diameter) at the Whistler high elevation site. Plot shows dV/dlogD as a composite from the SMPS and OPC. White areas indicate missing data.
(b) Time series of sub-micron and super micron total particle volume as determined from the SMPS and OPC.
(c) Sulphate and calcium concentrations from filter packs for particles less than 2 µm diameter.

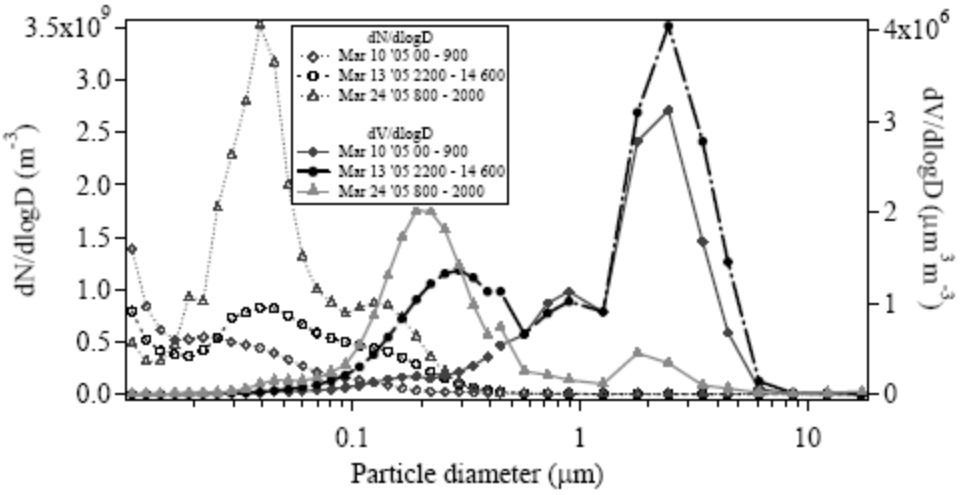

Figure 9: Number and volume distributions from the SMPS and OPC composites of Figure 8a averaged over selected periods (i) March 10 00:00 to 09:00, (ii) Mar13 22:00 to March 14 06:00, and (iii) Mar 24 08:00 to 20:00 LST.